Journal of Materials Chemistry

Cite this: *J. Mater. Chem.*, 2011, **21**, 12842

www.rsc.org/materials

PAPER

Silica boron–sulfuric acid nanoparticles (SBSANs): preparation, characterization and their catalytic application in the Ritter reaction for the synthesis of amide derivatives†

Ali Khalafi-Nezhad,*[a] Habib ollah Foroughi,[a] Mohammad Mahdi Doroodmand[ab] and Farhad Panahi*[a]

Received 17th March 2011, Accepted 7th June 2011
DOI: 10.1039/c1jm11154j

Among a number of different heterogeneous and homogeneous catalysts, silica boron–sulfuric acid nanoparticles (SBSANs) with both protic and Lewis acidic sites were shown to be the most active and recyclable catalyst in the Ritter reaction. Various amide derivatives were synthesized from alcohols and nitriles *via* a one-step and easy process in the presence of a catalytic amount of SBSAN at room temperature in solvent free conditions with excellent isolated yields. The silica boron–acid nanoparticles (SBANs) were regularly synthesized during the modification of the silica support by boric acid [$B(OH)_3$] during the chemical vapor deposition (CVD) process and subsequently, this material was reacted with chlorosulfonic acid ($ClSO_3H$) to obtain the SBSAN catalyst. The new catalyst was characterized using some different microscopic and spectroscopic techniques such as patterned X-ray diffraction (XRD), transmission electron microscopy (TEM), scanning electron microscopy (SEM), FT-Raman spectrometry and FT-IR spectroscopy. Thermal behavior of the SBSAN catalyst was also investigated by a thermogravimetric (TG) analyzer.

Introduction

In recent years modification of already existing synthetic methodologies in industrial and academic research has received greater attention. One of the major area of research is the development of heterogeneous catalysts for excellent chemical synthesis of materials.[1] For example, application of solid acids have been extensively studied and have been demonstrated to be highly efficient catalysts in organic transformations.[2] These heterogeneous catalysts possess some advantages including, easily application capabilities, decreased reactor and plant corrosion problems, and are more environmentally safe and available.[3–5] It is worth noting that the activity and selectivity of a heterogeneous catalyst is frequently decreased because the rate of reactant diffusion to the surface of catalyst is decreased.[6,7] It seems that, nanoparticles can be a good candidate as a support material, because the size of these materials is in the nanometre scale, the surface area will increase dramatically and will even be dispersible in solution to form an emulsion to increase the diffusion rate.[8,9] In this work, we prepared a new heterogeneous solid acid catalyst based on nanometre scale silica support with dual Lewis and protic acidic sites. To evaluate the catalytic performance of this new catalyst we checked the Ritter reaction as an acid catalyzed process. The preparation of amides from the reaction between alcohols or alkenes with nitriles in the presence of an acid is known as the Ritter reaction.[10,11] The Ritter reaction is an important transformation in organic synthesis because amide derivatives are present in natural, biological and industrial compounds as structural materials.[12–14] The reaction has been accomplished in harsh conditions and it required a strongly ionizing solvent and a stoichiometric amount of a strong acid such as sulfuric acid.[15] The synthetic applicability was limited in compounds in which their functional groups are not sensitive to acid.[16,17] On the other hand, the applicability of this reaction is limited to those capable of producing fairly stable carbenium ions.[18] Considering these limitations, application of alternative catalysts for synthetic improvement of this reaction is a matter of discussion and therefore various type of catalysts have been developed and introduced during the last decade. However, according to our knowledge, these catalysts often suffer from serious drawbacks such as toxicity, corrosiveness, cost, absence of recovery and reusability capability.[19–37] In this paper, we prepared silica boron–sulfuric acid nanoparticles (SBSANs) as a new heterogeneous catalyst. As shown in this study, SBSAN catalyst displays high reactivity in the Ritter reaction process in the absence of any promoter, and it can be further used for at least 8 runs. It seems that two catalytic sites of this catalyst in this reaction are engaged. In the current study, preparation, characterization and application of this catalyst in the Ritter reaction have been investigated in detail.

[a]*Department of Chemistry, Shiraz University, Shiraz, 71454, I. R. Iran. E-mail: khalafi@chem.susc.ac.ir; panahi@shirazu.ac.ir; Fax: +98-711-2280926; Tel: +98-711-2282380*
[b]*Nanotechnology Research Institute, Shiraz University, Shiraz, Iran*

† Electronic supplementary information (ESI) available: The ^1H NMR and ^{13}C NMR for all synthesized amides available in ESI. See DOI: 10.1039/c1jm11154j

Results and discussion

Catalyst preparation

Silica boron–sulfuric acid nanoparticles as a new catalyst were prepared based on the following operation (Scheme 1):

Catalyst characterization

The SBSAN catalyst was characterized using some different microscopic and spectroscopic techniques such as transmission electron microscopy (TEM), scanning electron microscopy (SEM), patterned X-ray diffraction (XRD), FT-IR spectroscopy and FT-Raman spectrometry. A thermogravimetric (TG) analyzer was also used for investigation of the thermal behavior of the SBSANs. In this study, the average diameter of the synthesized SBSANs based on the proposed procedure is evaluated to be ~38 nm. TEM image of the SBSAN catalyst (Fig. 1a) shows the SBSANs with near spherical morphology generated by the CVD process.

According to the SEM image (Fig. 2), it is clear that the silica nanoparticles are regular in shape and arranged in an approximately good orderly manner. The SEM image also confirmed this point that the SBSANs are produced with near spherical morphology.

The histogram revealing the size distributions of the SBSANs is shown in Fig. 3. The histogram was proposed according to the results obtained from the TEM and SEM images.

To explore further the chemically modification of the silica support with boron–sulfuric acid nanoparticles, the morphology of the catalyst was studied using XRD spectrometry. The XRD patterns of both silica and the SBSAN are shown in Fig. 4.

Comparison between the XRD pattern of SBSANs and pure silica reveals significant peaks positioned at $2\theta = 25.6$ and 28.1° for SBSANs. These two peaks are related to the presence of Si–O

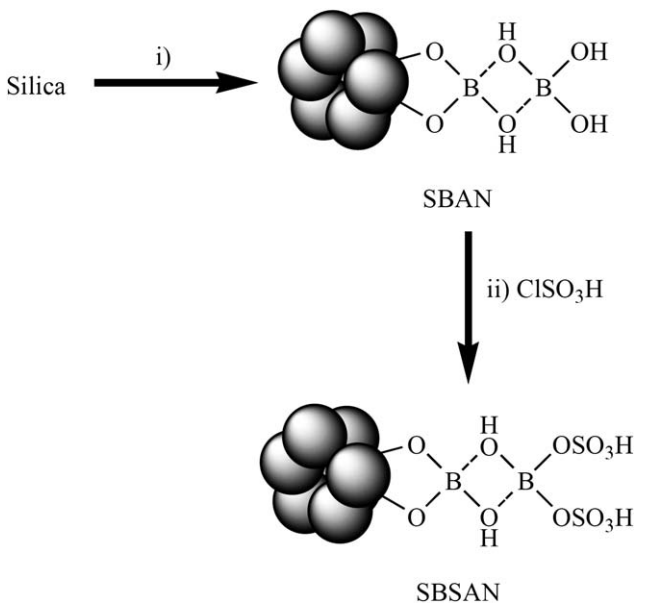

Scheme 1 Preparation of silica boron–acid nanoparticles (SBAN) and silica boron–sulfuric acid nanoparticles (SBSANs) catalyst. i) $B(OH)_3$, chemical vapor deposition (CVD) process (Ar, O_2); ii) $ClSO_3H$, r.t.

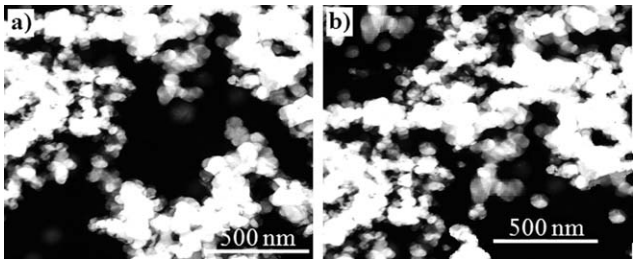

Fig. 1 TEM image of a) fresh SBSAN catalyst, and b) after 8 reuses.

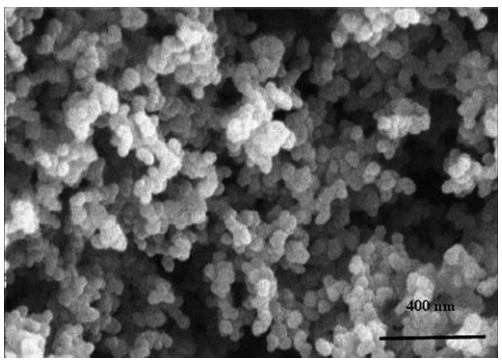

Fig. 2 SEM image of the SBSAN catalyst.

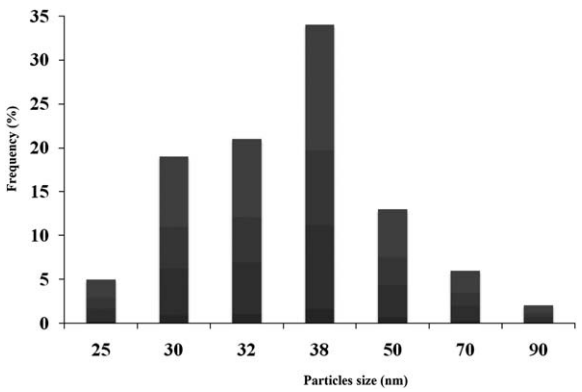

Fig. 3 Histogram representing the size distribution of the SBSAN catalyst.

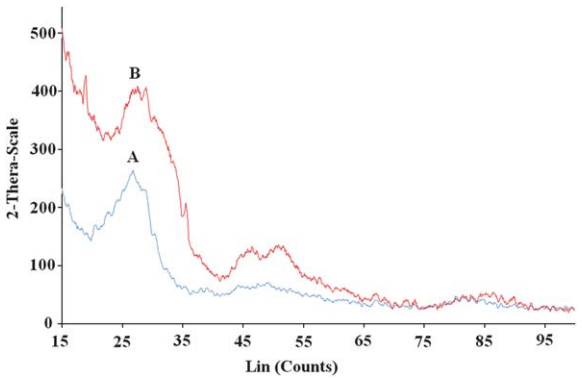

Fig. 4 XRD patterns of A) pure silica and B) the SBSANs.

and B–O bonds in the crystaline structure of the SBSANs respectively.[38]

According to the obtained data from the TEM, SEM and XRD we can say with sure that this catalyst has a nanostructural nature, but these techniques have not much information about the catalyst's chemical bonds and functional groups. Thus, for further identification of the catalyst and characterization of the chemical bonds, we need to other techniques such as FT-IR spectroscopy and Raman spectrometry.

The FT-IR spectra of the both pure silica and the SBSANs are shown in Fig. 5.

In agreement with the FT-IR spectra, the peaks positioned at ~609 and ~1632 cm^{-1} are related to the formation of B–O–B and B–O bands, respectively.[39] The band at 1122 cm^{-1} was attributed to the Si–O–Si stretching vibrations in the SBSAN catalyst.[40] The stretching vibrations of B–OH bonds were observed at ~1450 and 1350 cm^{-1}. The bond at ~710 cm^{-1}, is probably related to the B–O–Si bond.[40] The asymmetric and symmetric stretching of the O=S=O fragment was observed at 1320 and 1198 cm^{-1} respectively. The FT-IR spectrum gives a good indication of the successful preparation of the SBSANs.

The formation of B–O as well as B–O–B bonds was also approved using Raman spectrometry. According to the Raman spectrum (Fig. 6), sharp peaks positioned at ~480 cm^{-1} and ~590 cm^{-1} belong to the formation on B–O and B–O–B bonds, respectively.[38] This reveals that, the proposed procedure is considered as a good method for modification of the silica support for doping different functional groups such as boron sulfuric acid.

As you can see, the FT-IR and Raman techniques demonstrate as well the chemical bonds and functional groups in the structure of the SBSAN catalyst. Since, in the SBSAN catalyst both B–O and B–O–B bonds are evident, it can be proposed that a complex nature for boron atoms exists in this material (boronate complex) (Fig. 7). Considering this boronate complex we can say that the active site of this catalyst could be the proton counter ion of this complex. Since, these protons possess a more stable conjugated base, this catalyst generates an efficient acidic environment for reactions to be accomplish in, under mild conditions.

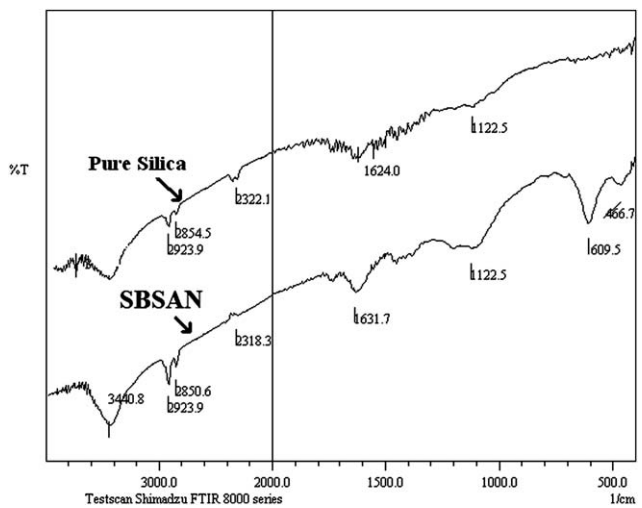

Fig. 5 Comparison between FT-IR spectra of pure silica and the SBSANs.

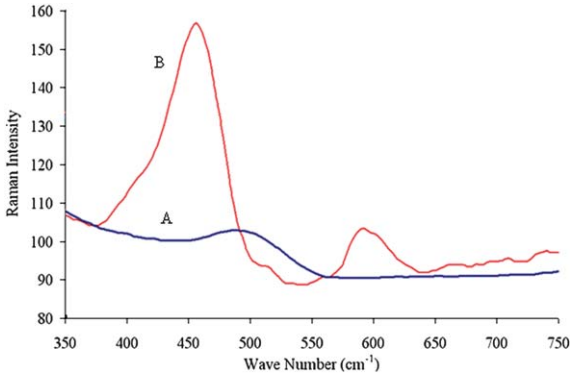

Fig. 6 The raman spectra of A) pure silica and B) SBSAN catalyst.

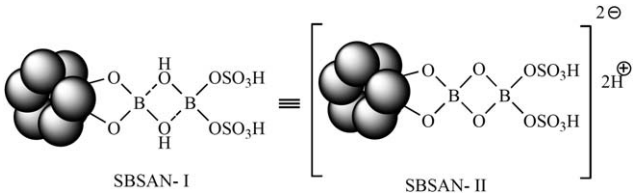

Fig. 7 The proposed structure for the SBSAN catalyst.

In this study, the amounts of boron atoms doped on activated silica were evaluated using a TG analysis instrument. As clearly observed according to the thermogram (Fig. 8), a decrease in the weight percentage of the catalyst at temperatures to ~470 °C is due to the decomposition of sulfuric acid and oxidation of boron atoms. Also, decreases in the weight percentage of the catalyst at temperatures up to ~900 °C is related to decomposition of the silica support. In addition, the end parts of the thermogram (Fig. 8) reveals the amounts of boron oxide and indirectly shows the amounts of boron atoms doped on the silica support. This was estimated to be ~6.11%, (w/w).

Also the active surface area of the boron sulfuric-acid doped on silica was investigated *via* investigation of the nitrogen adsorption of both silica and silica boron sulfuric acid nano-particle. The data as presented in Fig. 9 reveals the nitrogen adsorption isotherm (at 25 °C) using the TG analyzer.

Based on the results obtained from the nitrogen adsorption isotherms (Fig. 9), the boron doping process, there was a significant increase to ~279 $m^2\ g^{-1}$ in the active surface area of

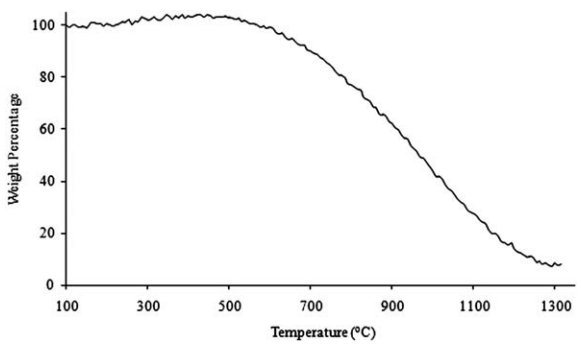

Fig. 8 Thermogram of SBSANs.

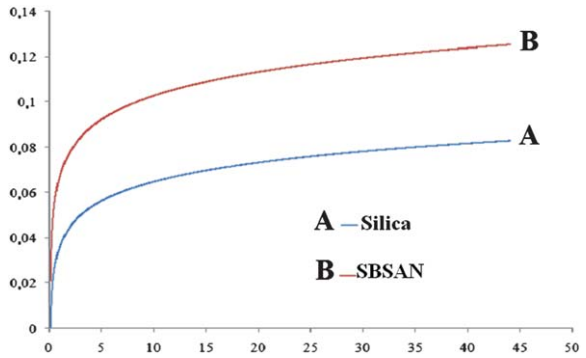

Fig. 9 Nitrogen adsorption behaviour of A) silica and B) SBSANs at 25 °C.

the silica, revealing highly improved catalytic activity of the catalyst during its application in the synthesis of organic products.

Also, elemental analysis revealed that, the sulfur content was evaluated to be ~6.05. This result is in good agreement with the obtained loaded catalyst according to the TG analyzer.

The Ritter reaction

The SBSAN catalyzed Ritter reaction between *t*-butyl alcohol and benzonitrile was chosen as a simple model reaction to evaluate the effects of solvent, temperature and the amounts of catalyst. Optimization conditions are shown in Table 1.

In our initial selection, we used boric acid [$B(OH)_3$] in ethanol for the reaction between benzonitrile and *t*-butyl alcohol, and *N*-*tert*-butylbenzamide was obtained with trace isolated yield (Table 1, entry 1). Then, the effect of solvent was investigated for this reaction and we found that in solvent free conditions, the yield of product was enhanced to 28% after 24 h at 100 °C (Table 1, entry 3). It can be seen that, in a non-coordinate solvent such as CH_2Cl_2, the amount of product has increased to some extent. This could be due to the availability of the acidic Lewis sites of B $(OH)_3$ in these solvents (Table 1, entry 2). It seems that the silica boric acid nanoparticle catalyst as a supported boric acid is more effective than boronic acid (Table 1, entry 4). This is probably due to increasing the catalyst surface in SBAN than in boric acid and also the effect of the silica substrate in the progress of this reaction. Continuing our study, we use silica sulfuric acid (SSA)[41] for this reaction and in the best examined condition (solvent free and at a temperature of 100 °C) the isolated yield of product obtained was 60% (Table 1, entry 8). These results prompted us to apply SSA and $B(OH)_3$ simultaneously in the reaction. Interestingly, the mixture of $B(OH)_3$ and SSA in solvent free conditions and at 100 °C was showed good reactivity for this reaction and in shorter reaction times, and a small increase in the amount of product was observed (Table 1, entry 9). Regarding this point, we decided to prepare the SBSAN catalyst for use in this reaction. This catalyst shows very interesting results in the Ritter reaction which was not comparable with the other solid acids. The catalyst activity of SBSANs, presumably is related to: 1) the boron Lewis acidic site, 2) the sulfuric acid proton and 3) nanostructured nature of the silica support. You can see in Table 1 that, reactivity of this catalyst was limited to coordinate solvents, for example in ethanol and CH_2Cl_2, the yield of product were obtained 56% and 78%, respectively (Table 1, entries 10 and 11). Also, in solvent free conditions, SBSAN catalyst was shown to have high reactivity and the desired product was obtained in a short reaction time with excellent isolate yield (92%) (Table 1, entry 12). These results, certainly confirmed that the reactivity of this catalyst depends on the existence of its two acidic sites and boron atom, and they play effective roles in the catalytic activity of SBSAN catalyst. This point should also be considered that in the SBSAN catalyst the boron atom is connected to two electron withdrawing groups (OSO_3H), and so the Lewis acidity of boron atom in this catalyst has somewhat increased. With increasing

Table 1 Study of various conditions for the Ritter reaction of *t*-butyl alcohol with benzonitrile[a]

Entry	Catalyst[b]	Solvent[c]	Temp. (° C)	Time (h)	Yield (%)[d]
1	$B(OH)_3$	EtOH	80	24	Trace
2	$B(OH)_3$	CH_2Cl_2	60	24	20
3	$B(OH)_3$	None	100	24	28
4	SBAN	None	100	24	45
5	SSA	Ethanol	80	12	43
6	SSA	CH_2Cl_2	60	12	55
7	SSA	None	r.t	2	20
8	SSA	None	100	12	60
9	SSA/$B(OH)_3$	None	100	5	68[e]
10	SBSAN	EtOH	80	2	56
11	SBSAN	CH_2Cl_2	60	2	78
12	SBSAN	None	r.t	0.5	92[f], 90[g], 83[h], 62[i]
13	SBSAN	None	40	0.25	92
14	SBSAN	None	80	0.2	95
15	SBSAN	None	100	0.2	97
16	$Bi(OTf)_3$	H_2O	100	2	38
17	H_2SO_4	ACOH	80	5	44
18	I_2	CH_2Cl_2	60	10	35
19	$FeCl_3$	None	100	5	33

[a] Reaction conditions: *t*-butyl alcohol (1mmol), benzonitrile (1mmol). [b] 0.1 g of catalysts was used. [c] 5.0 mL of solvent was used. [d] Isolated yield. [e] 0.05g of SSA and 0.05g of $B(OH)_3$ were used. [f] 0.15 g of SBSAN was used. [g] 0.1 g of SBSAN was used. [h] 0.075 g of SBSAN was used. [i] 0.05 g of SBSAN was used.

the amount of catalyst (0.15 g per 1.0 mmol of benzonitrile) the yield of product does not much change. Whereas, after reducing the amount of catalyst (0.075 g per 1.0 mmol of benzonitrile) a significant decrease was observed in the yield of product (Table 1, entry 12). These results were shown that the catalytic amount of SBSAN catalyst is required for promotion of Ritter reaction.

During our optimization studies, various temperatures were examined and it was found that, the temperature has a poor effect in terms of the reaction rate, and isolated yield, but it seems that, the decrease in the temperature results in a decrease in the yield of product (Table 1, entries 13, 14 and 15). Since, the amount of product in room temperature is comparable with other temperatures (40, 80 and 100 °C), this temperature was selected for optimum reaction conditions (Table 1, entry 12). For comparison, under the above conditions (solvent free and room temperature), $Bi(OTf)_3$,[42] H_2SO_4,[43] I_2,[44] and $FeCl_3$[45] were used, but the reaction did not performed and the yield of product was not comparable with SBSANs (Table 1, entries 16–19). According to Table 1, in the presence of a catalytic amount of SBSAN catalyst and in solvent free conditions at room temperature the Ritter reaction can be accomplished. Various amide derivatives in excellent isolated yields were synthesized under these conditions, and the results are summarized in Table 2.

The generality and the scope of this protocol were to evaluate for both aromatic and aliphatic alcohols, and a variety of synthetic nitriles were synthesized using SBSAN catalyst. In all these cases, the Ritter reaction proceeded quickly and the desired products were obtained in the excellent yields. For example the reaction of CH_3CN with Ph_2CHOH in the presence of 0.10 g of SBSAN produced the *N*-benzhydrylacetamide in 90% isolated yield after only 15 min. The yields of all amides were more than 90%.

We also, checked the reaction of benzonitrile with alkenes and alcohol acetates in the presence of SBSAN catalyst and interesting results were obtained. As can be seen in Table 3, this catalyst also provides an efficient acidic condition for these substrates to undergo the Ritter reaction. For these substrates, the corresponding amides were obtained with excellent isolated yields.

In general, in the presence of SBSAN catalyst the reaction has advantages such as the following: i) the Ritter reaction carried out at room temperature and in solvent free conditions, ii) it avoids the use of corrosive and toxic reagents, and iii) a catalytic amount of SBSANs was used. Therefore this catalyst has made this reaction eco-friendly. Furthermore, this reaction is useful to prepare amide derivatives, which may be useful in the preparation of the amines by hydrolysis.

We also proposed the following mechanism for the Ritter reaction in the presence of SBSAN catalyst in a boronate complex form considered to the reported mechanism in the literature[46] and based on obtained results during study of this catalyst in Ritter reaction (Scheme 2).

The possibility of recycling the catalyst was tested using the reaction of *t*-butyl alcohol with benzonitrile under optimized conditions [benzonitrile (1 mmol), *t*-butyl alcohol (1 mmol) and SBSANs (0.1 g)]. When the reaction was completed, some water was added to reaction media and the reaction mixture was washed with dicholoromethane and then the catalyst separated by simple filtration. For losing co-ordinate solvents, the recycled catalyst was heated in an oven (at 100 °C for 2h) and finally was saved for the next operation. The recycled catalyst could be reused seven times without any treatment (Fig. 10).

After eight times of reusability we checked the sulfur content of SBSAN catalyst using CHNS analysis instrument, and the results were shown that only 1.8% of sulfur was lost. Also the TEM image of catalyst was shown that the morphology of catalyst after being recycled 8 times does not changed significantly (Fig. 1b). These results are in good agreements with the catalytic activity of the SBSANs after each recovery and you can see that no observation of any appreciable loss in the catalytic activity of SBSAN catalyst was detected.

Conclusions

In this study, silica–boron acid nanoparticles (SBAN) were successfully synthesized during the modification of silica by boric acid using a CVD process. Sulfonation of the SBAN using chlorosulfonic acid results in silica boron–sulfuric acid as a novel heterogeneous catalyst with dual Lewis-protic acidic sites. The synthetic usefulness of this heterogeneous catalyst in the synthesis of amide derivatives *via* the Ritter reaction was demonstrated. The target products ranging from **a–m** were obtained in excellent yields and short reaction times. Furthermore, SBSANs possess some advantages over other acidic catalysts, which have been used so far in research laboratories, such as improved safety, and are non-volatile, non-corrosive and reusable and with efficient effectiveness. A further valuable aspect of the use of SBSAN is its high activity in non-donor solvents and especially in solvent free conditions.

Experimental section

1. Chemical, instrumentation and analysis

Chemicals were purchased from Fluka, Merck and Aldrich Chemical Companies. For recorded ^1H NMR spectra we used a Brucker (500MHZ) Avanc DRX in pure deuterated DMSO-d_6 and $CDCl_3$ solvents with tetramethylsilane (TMS) as the internal standard. Mass spectra were recorded on a FINNIGAN-MAT 8430 mass spectrometer operating at 70 eV. FT-IR spectroscopy (Shimadzu FT-IR 8300 spectrophotometer), was employed for characterization of the compounds. The scanning electron micrograph for SBSAN catalyst was obtained by SEM instrumentation (SEM, XL-30 FEG SEM, Philips, at 20 kV) and also transmission electron microscopy (TEM) was obtained using TEM apparatus (CM-10-philips, 100 kV). The thermogravimetry analysis (TGA) of the samples was analyzed using a lab-made TGA instrument. The Raman spectra was also taken using a FT-Raman spectrometer (Thermo Nicolet Almega dispersive). Melting points were determined in open capillary tubes in a Barnstead Electrothermal 9100 BZ circulating oil melting point apparatus. The reaction monitoring was accomplished by TLC on silica gel PolyGram SILG/UV254 plates. Column chromatography was carried out on columns of silica gel 60 (70–230 mesh).

Table 2 The Ritter reaction of nitriles with alcohols in the presence of SABSAN[a]

Entry	Nitrile	Alcohol	Product	Time (min)	Yield (%)[b]
1	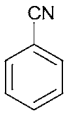	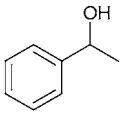	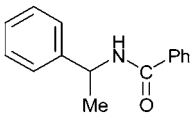 **(a)**	15	93
2	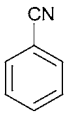		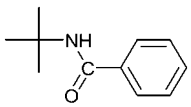 **(b)**	15	92
3	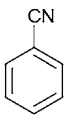	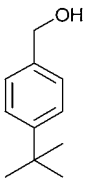	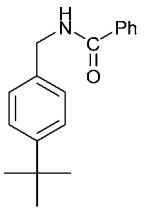 **(c)**	20	95
4	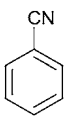	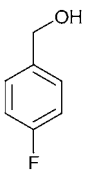	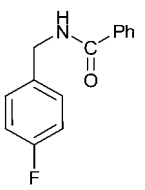 **(d)**	25	90
5		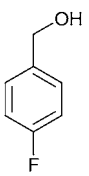	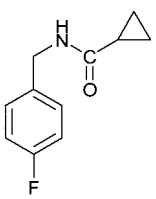 **(e)**	20	92
6		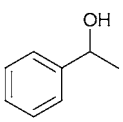	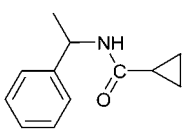 **(f)**	10	95
7		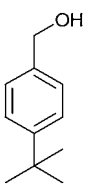	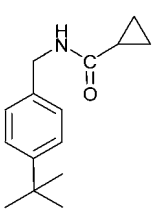 **(g)**	15	93
8			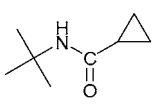 **(h)**	15	97

Table 2 (*Contd.*)

Entry	Nitrile	Alcohol	Product	Time (min)	Yield (%)[b]
9			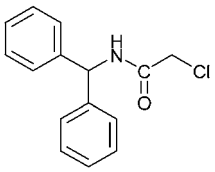 (i)	25	90
10			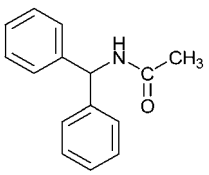 (j)	15	90
11	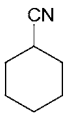		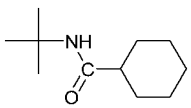 (k)	20	91
12	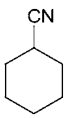	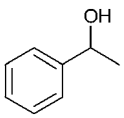	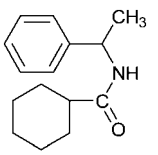 (l)	10	96
13			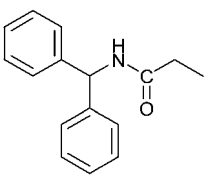 (m)	20	92

[a] Reaction conditions: alcohol (1.0 mmol), nitrile (1.0 mmol) and SBSAN (0.1 g). [b] Isolated yield.

2. Preparation of SBANs

In this study, chemical vapor deposition (CVD) process was used for doping of boron species on a silica support. For this purpose, briefly, a mixture of Ar, O_2 and the aerosols of the aqueous solution of boric acid ($\sim$2.0 g mL^{-1}) were introduced to the solid silica supports positioned inside a quartz tube located in a tubing furnace at temperatures of $\sim$600 °C. This process resulted in the formation of SBANs.

3. Preparation of SBSANs

In a 100 mL suction flask that was equipped with a dropping funnel containing chlorosulfonic acid (7.64 g, 0.066 mole) and a gas inlet tube for conducting HCl gas over an adsorbing solution (10% NaOH). Then, 10 g of SBANs were charged in to the flask. Chlorosulfonic acid was added drop-wise over a period of 60 min at room temperature. HCl gas evolved from the reaction vessel immediately. When the addition was completed, the mixture was stirred for 30 min under vacuum pressure. The SBSANs were obtained (15.1 g) as a white solid.

4. General procedure for SBSAN-catalyzed amidation of alcohols

Into a canonical flask (25.0 mL) a mixture of alcohol (1.0 mmol), nitrile (1.0 mmol) and SBSAN (0.1 g) were stirred at room temperature. The reactions were monitored by TLC. Stirring was continued until the consumption of the starting materials based on reaction time in Table 2. After completion of the reaction, some water was added to a flask and then the mixture was washed with dichlorometane and the catalyst separated by simple filtration. The solvent was removed under reduced pressure and the product was purified by silica gel column chromatography employing methanol/ethyl acetate as the eluent, affording the pure corresponding amide.

Table 3 The Ritter reaction of nitriles with alkenes and acetated alcohols in the presence of SBSANs[a]

Entry	Nitrile	Alkene/acetate	Product	Time (min)	Yield (%)[b]
1	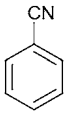		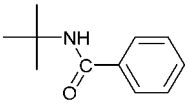 **(b)**	20	91
2	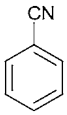	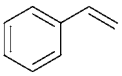	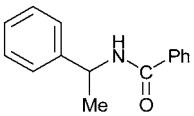 **(a)**	30	95
3	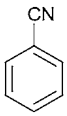		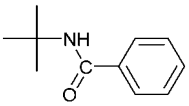 **(b)**	45	90
4	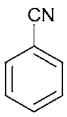	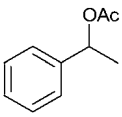	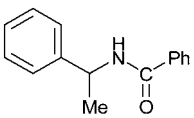 **(a)**	60	93

[a] Reaction conditions: acetated alcohol or alkene (1.0 mmol), benzonitrile (1.0 mmol) and SBSAN (0.1 g). [b] Isolated yield.

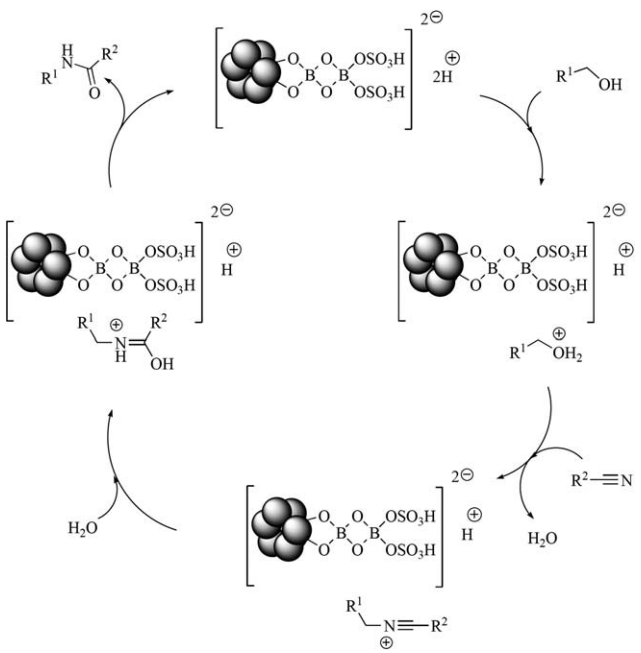

Scheme 2 Proposed mechanism for the Ritter reaction using SBSAN catalyst.

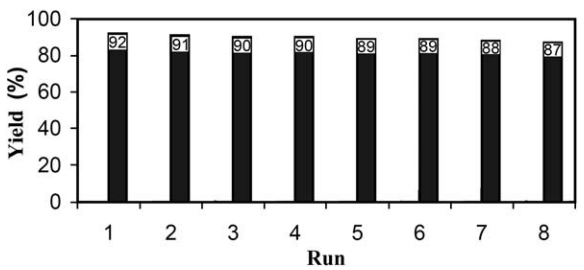

Fig. 10 Catalytic recovery times of SBSAN catalyst for eight runs.

5. The spectral data for synthesized amides

5.1. ***N*-(1-Phenylethyl) benzamide (a).** White color, mp 115–116 °C. MS: *m*/*z* (%): 225.11 (68), 120.05 (42), 105.07 (22), 105.03 (35), 77.04 (54). IR (KBr) (cm^{-1}): 3300, 1625, 1420. ^1H NMR (500 MHz, $CDCl_3$/TMS) δ (ppm): 1.65 (d, $J = 6.9$ Hz, 3H), 5.39 (q, $J = 2.3$, 6.9 Hz, 1H), 6.51 (brs, 1H), 7.30–7.54 (m, 8H), 7.82 (d, $J = 7.4$ Hz, 2H). ^{13}C NMR (125 MHz, $CDCl_3$/TMS) δ (ppm): 22.2, 49.6, 126.7, 127.4, 127.9, 129.0, 129.2, 131.9, 135.0, 143.6, 167.0. Anal. calcd for $C_{15}H_{15}NO$ (225.29): C, 79.97; H, 6.71; N, 6.22. Found: C, 79.93; H, 6.69; N, 6.20.

5.2. ***N*-*tert*-Butylbenzamide (b).** White color, mp 133–134 °C. MS: *m*/*z* (%):177.11 (87), 106.05 (39), 73.07 (61). IR (KBr): ν = 3330, 1630, 1410 cm^{-1}. ^1H NMR (500 MHz, $CDCl_3$/TMS) δ (ppm): 1.51 (s, 9H), 5.95 (brs, 1H), 7.44 (m, 2H), 7.51 (t, $J = 7.3$ Hz, 1H), 7.75 (d, $J = 7.1$ Hz, 2H). ^{13}C NMR (125 MHz, $CDCl_3$/TMS) δ (ppm): 29.3, 52.0, 127.1, 128.8, 131.5, 136.4, 167.3. Anal. calcd for $C_{11}H_{15}NO$ (177.24): C, 74.54; H, 8.53; N, 7.90. Found: C, 74.51; H, 8.50; N, 7.92.

5.3. ***N*-(4-*tert*-Butylbenzyl)benzamide (c).** White color, mp 105–106 °C. MS: *m*/*z* (%): 267.15 (64), 163.13 (56), 148.11 (62), 106.13. (33). IR (KBr): ν = 3300, 1620, 1300 cm^{-1}. ^1H NMR (500 MHz, $CDCl_3$/TMS) δ (ppm): 1.37 (s, 9H), 4.56 (d, $J = 5.5$ Hz,

2H), 6.58 (brs, 1H), 7.33–7.46 (m, 6H), 7.53 (t, $J = 7.3$ Hz, 1H), 7.75 (d, $J = 7.4$ Hz, 2H). ^{13}C NMR (125 MHz, $CDCl_3$/TMS) δ (ppm): 1.5, 31.8, 34.0, 44.3, 126.1, 127.4, 128.6, 128.8, 129.0, 131.9, 135.6, 151.1, 167.8. Anal. calcd for $C_{18}H_{21}NO$ (267.37): C, 80.86; H, 7.92; N, 5.24. Found: C, 80.84; H, 7.89; N, 5.23.

5.4. *N*-(4-Fluorobenzyl)benzamide (d). White color, mp 114–116 °C. MS: *m*/*z* (%): 229.08 (81), 109.05 (38), 120.05 (62), 77.04 (36). IR (KBr): $\nu = 3290$, 1620, 1415 cm^{-1}. ^{1}H NMR (500 MHz, $CDCl_3$/TMS) δ (ppm): 4.59 (d, $J = 4.9$ Hz, 2H), 6.56 (brs, 1H), 7.01 (t, $J = 8.1$ Hz, 2H), 7.30 (m, 2H), 7.40–7.49 (m, 3H) 7.78 (d, $J = 7.1$ Hz, 2H). ^{13}C NMR (125 MHz, $CDCl_3$/TMS) δ (ppm): 43.8, 115.9, 116.1, 127.4, 129.0, 129.9, 130.0, 132.0, 134.5, 134.9. Anal. calcd for $C_{14}H_{12}FNO$ (229.25): C, 73.35; H, 5.28; N, 6.11. Found: C, 73.33; H, 5.25; N, 6.09.

5.5. *N*-(4-Fluorobenzyl)cyclopropanecarboxamide (e). White color, mp 117–119 °C. MS: *m*/*z* (%):193.07 (base peak), 125.05 (56), 70.02 (43). IR (KBr): $\nu = 3290$, 1625, 1390 cm^{-1}. ^{1}H NMR (500 MHz, $CDCl_3$/TMS) δ (ppm): 0.75 (dt, $J = 10.7$, 3.5 Hz, 2H), 1.0 (dt, $J = 7.4$, 3.0 Hz, 2H), 1.33–135 (m, 1H), 4.41 (d, $J = 5.7$ Hz, 2H), 5.92 (brs, 1H), 6.98–7.03 (m, 2H), 7.24–7.27 (m, 2H). ^{13}C NMR (125 MHz, $CDCl_3$/TMS) δ (ppm): 7.7, 15.2, 43.5, 115.8, 116.0, 129.8, 129.9, 134.8, 163.6, 173.9. Anal. calcd for $C_{11}H_{12}FNO$ (193.22): C, 68.38; H, 6.26; N, 7.25. Found: C, 68.34; H, 6.21; N, 7.22.

5.6. *N*-(1-Phenylethyl)cyclopropanecarboxamide (f). White color, mp 102–103 °C. MS: *m*/*z* (%): 231.15 (69), 162.13 (51), 147.12 (20), 84.04 (28). IR (KBr): $\nu = 3300$, 1635, 1390 cm^{-1}. ^{1}H NMR (500 MHz, $CDCl_3$/TMS) δ (ppm): 1.18–1.24 (m, 4H), 1.31 (s, 9H), 1.34–1.80 (m, 6H), 1.94 (m, 1H), 5.23 (brs, 1H). ^{13}C NMR (125 MHz, $CDCl_3$/TMS) δ (ppm): 7.6, 15.2, 31.8, 34.9, 44.0, 126.1, 128.1, 135.9, 151.0, 173.7. Anal. calcd for $C_{15}H_{21}NO$ (231.33): C, 77.88; H, 9.15; N, 6.05. Found: C, 77.86; H, 9.13; N, 6.04.

5.7. *N*-(4-*tert*-Butylbenzyl)cyclopropanecarboxamide (g). White color, mp 141–142 °C. MS: *m*/*z* (%): 141.11 (49), 85.04 (57), 58.07 (61), 44.06 (28). IR (KBr): $\nu = 3290$, 1635, 1390 cm^{-1}. ^{1}H NMR (500 MHz, $CDCl_3$/TMS) δ (ppm): 0.69 (dt, $J = 10.7$, 3.5 Hz, 2H), 0.92 (dt, $J = 7.1$, 3.0 Hz, 2H), 1.25–130 (m, 1H), 1.38 (s, 9H), 5.53 (brs, 1H). ^{13}C NMR (125 MHz, $CDCl_3$/TMS) δ (ppm): 7.0, 15.8, 29.4, 15.6, 173.0. Anal. calcd for $C_8H_{15}NO$ (141.21): C, 68.04; H, 10.71; N, 9.92. Found: C, 68.01; H, 10.68; N, 9.90.

5.8. *N*-*tert*-Butylcyclopropanecarboxamide (h). White color, mp 123–125 °C. MS: *m*/*z* (%):259.06 (83), 225.11 (37), 183.23 (21) 168.21 (60), 93.50 (34). IR (KBr): $\nu = 3230$, 1635, 1395 cm^{-1}. ^{1}H NMR (500 MHz, $CDCl_3$/TMS) δ (ppm): 4.19 (s, 2H), 6.26 (d, 1H, $J = 8.2$ Hz), 7.19 (brs, 1H), 7.24 (d, $J = 4.0$ Hz, 4H), 7.29 (t, $J = 7.2$ Hz, 2H), 7.35 (t, $J = 7.2$ Hz, 4H). ^{13}C NMR (125 MHz, $CDCl_3$/TMS) δ (ppm): 43.1, 57.6, 127.7, 128.2, 129.2, 141.2, 165.4. Anal. calcd for $C_{15}H_{14}ClNO$ (259.73): C, 69.36; H, 5.43; N, 5.39. Found: C, 69.30; H, 5.40; N, 5.37.

5.9. *N*-Benzhydryl-2-chloroacetamide (i). White color, mp 144–145 °C. MS: *m*/*z* (%): 225.12 (70), 168.10 (38), 59.04 (52). IR (KBr): $\nu = 3350$, 1630, 1310 cm^{-1}. ^{1}H NMR (500 MHz, $CDCl_3$/TMS) δ (ppm): 2.04 (s, 3H), 6.15 (brs, 1H), 6.25 (d, $J = 5.0$ Hz, 1H), 7.21–7.35 (m, 10H). ^{13}C NMR (125 MHz, $CDCl_3$/TMS) δ (ppm): 23.8, 57.4, 127.7, 127.8, 127.9, 128.8, 129.1, 141.9, 169.5. Anal. calcd for $C_{15}H_{15}NO$ (225.29): C, 79.97; H, 6.71; N, 6.22. Found: C, 79.94; H, 6.68; N, 6.19.

5.10. *N*-Benzhydrylacetamide (j). White color, mp 110–111 °C. MS: *m*/*z* (%): 183.15 (79), 111.06 (47), 83.09 (16), 72.08 (31). IR (KBr): $\nu = 3300$, 1635, 1390 cm^{-1}. ^{1}H NMR (500 MHz, $CDCl_3$/TMS) δ (ppm): 1.18–1.24 (m, 4H), 1.31 (s, 9H), 1.34–1.80 (m, 6H), 1.94 (m, 1H), 5.23 (brs, 1H). ^{13}C NMR (125 MHz, $CDCl_3$/TMS) δ (ppm): 26.2, 29.3, 30.2, 46.7, 51.2, 176.0. Anal. calcd for $C_{11}H_{21}NO$ (183.29): C, 72.08; H, 11.55; N, 7.64. Found: C, 72.03; H, 11.51; N, 7.62.

5.11. *N*-*tert*-Butylcyclohexanecarboxamide (k). White color, mp 107–109 °C. MS: *m*/*z* (%): 231.15 (83), 126.09 (37), 105.07 (24), 83.09 (44). IR (KBr): $\nu = 3320$, 1640, 1430 cm^{-1}. ^{1}H NMR (500 MHz, $CDCl_3$/TMS) δ (ppm): 1.21–1.25 (m, 3H), 1.40–1.88 (m, 10H), 2.03–2.09 (m, 1H), 5.09–5.15 (m, 1H), 5.67 (brs, 1H), 7.23–7.34 (m, 5H). ^{13}C NMR (125 MHz, $CDCl_3$/TMS) δ (ppm): 22.2, 26.7, 30.0, 30.1, 46.0, 48.7, 126.5, 127.7, 129.1, 143.9 and 175.5. Anal. calcd for $C_{15}H_{21}NO$ (231.33): C, 77.88; H, 9.15; N, 6.05. Found: C, 77.82; H, 9.11; N, 6.04.

5.12. *N*-(1-Phenylethyl)cyclohexanecarboxamide (l). White color, mp 147–148 °C. MS: *m*/*z* (%): 239.14 (77), 167.09 (45), 72.04 (14), 57.03 (54). IR (KBr): $\nu = 3300$, 1635, 1380 cm^{-1}. ^{1}H NMR (500 MHz, $CDCl_3$/TMS) δ (ppm): 1.17 (t, $J = 7.5$ Hz, 3H), 2.27 (q, $J = 2.1$, 7.5 Hz, 2H), 6.15 (brs, 1H), 6.26 (d, $J = 8.0$ Hz, 1H), 7.22 (d, $J = 7.1$ Hz, 4H), 7.26 (t, $J = 7.2$ Hz, 2H), 7.32 (t, $J = 7.1$ Hz, 4H). ^{13}C NMR (125 MHz, $CDCl_3$) δ (ppm): 10.3, 30.1, 57.2, 127.7, 127.8, 128.8, 129.1, 124.1, 173.2. Anal. calcd for $C_{16}H_{17}NO$ (239.31): C, 80.30; H, 7.16; N, 5.85. Found: C, 80.26; H, 7.11; N, 5.83.

5.13. *N*-Benzhydrylpropionamide (m). White color, mp 112–113 °C. MS: *m*/*z* (%): 191.12 (55), 100.08 (62), 91.05 (37), 72.08 (21). IR (KBr): $\nu = 3290$, 1620, 1415 cm^{-1}. ^{1}H NMR (500 MHz, $CDCl_3$/TMS) δ (ppm): 1.32 (s, 9H), 3.48 (s, 2H), 5.20 (brs, 1H), 7.23–7.26 (m, 3H), 7.32–7.35 (m, 2H), ^{13}C NMR (125 MHz, $CDCl_3$/TMS) δ (ppm): 29.1, 45.3, 51.6, 127.5, 129.3, 129.7, 135.9, 170.7. Anal. calcd for $C_{12}H_{17}NO$ (191.27): C, 75.35; H, 8.96; N, 7.32. Found: C, 75.31; H, 8.91; N, 7.29.

Acknowledgements

We acknowledge Shiraz University for partial support of this work. Also, we are thankful to Dr Reza Yousefi for helpful comments.

Notes and references

1 D. Choudhary, S. Paul, R. Gupta and J. H. Clark, *Green Chem.*, 2006, **8**, 479.
2 J. A. Melero, R. V. Grieken and G. Morales, *Chem. Rev.*, 2006, **106**, 3790.
3 B. Karimi and D. Zareyee, *Org. Lett.*, 2008, **10**, 3989.
4 W. M. Van Rhijn, D. E. De Vos, B. F. Sels, W. D. Bossaert and P. A. Jacobs, *Chem. Commun.*, 1998, 317.

5 I. K. Mbraka, D. R. Radu, V. S.-Y. Lin and B. H. Shanks, *J. Catal.*, 2003, **219**, 329.
6 P. D. Stevens, J. D. Fan, H. M. R. Gardinmalla and M. Yen, *Org. Lett.*, 2005, **7**, 2085.
7 T. J. Yoon, W. Lee and Y. S. Oh, *New J. Chem.*, 2003, **27**, 227.
8 J. Fan, S. Chen and Y. Gao, *Colloids Surf., B*, 2003, **28**, 199.
9 A. J. Kell, D. L. B. Stringle and M. S. Workentin, *Org. Lett.*, 2000, **2**, 3381.
10 J. J. Ritter and P. P. Minieri, *J. Am. Chem. Soc.*, 1948, **70**, 4045.
11 F. R. Benson and J. J. Ritter, *J. Am. Chem. Soc.*, 1949, **71**, 4128.
12 N. P. Gerasimova, N. A. Nozhnin, V. V. Ermolaeva, A. V. Ovchinnikova, Y. A. Moskvichev, E. M. Alov and A. S. Danilova, *Mendeleev Commun.*, 2003, **13**, 82.
13 J. T. Puche, E. Marcucci, E. Prats-Alfonso, N. B. Puxan and F. Albericio, *J. Med. Chem.*, 2009, **52**, 834.
14 P. Chand, Y. S. Babu, S. Bantia, S. Rowland, A. Dehghani, P. L. Kotian, T. L. Hutchison, S. Ali, W. Brouillette, Y. El-Kattan and T. H. Lin, *J. Med. Chem.*, 2004, **47**, 1919.
15 A. Agrawal, C. A. F. De Oliveira, Y. Cheng, J. A. Jacobsen, J. A. McCammon and S. M. Cohen, *J. Med. Chem.*, 2009, **52**, 1063.
16 K. V. Emelen, T. De Wit, G. J. Hoornaert and F. Compernolle, *Org. Lett.*, 2000, **2**, 3083.
17 F. Maertens, A. V. den Bogaert, F. Compernolle and G. J. Hoornaert, *Eur. J. Org. Chem.*, 2004, 4648.
18 R. Sanz, A. Martinez, V. Guilarte, J. M. Alvarez-Gutierrez and F. Rodriguez, *Eur. J. Org. Chem.*, 2007, 4642.
19 K. Laxma Reddy, *Tetrahedron Lett.*, 2003, **44**, 1453.
20 G. C. Gullickson and D. E. Lewis, *Synthesis*, 2003, 681.
21 M. Shi and G. Q. Tian, *Tetrahedron Lett.*, 2006, **47**, 8059.
22 T. Maki, K. Ishihara and H. Yamamoto, *Tetrahedron*, 2007, **63**, 8059; K. V. Katkar, P. S. Chaudhari and K. G. Akamanchi, *Green Chem.*, 2011, **13**, 835.
23 E. Callens, A. J. Burton and A. G. M. Barrett, *Tetrahedron Lett.*, 2006, **47**, 8699; S. Sakaguchi, T. Hirabayashi and Y. Ishii, *Chem. Commun.*, 2002, 516.
24 R. M. A. Pinto, J. A. R. Salvador and C. Le Roux, *Synlett*, 2006, 2047; A. Jirgensons, V. Kauss, A. F. Mishnev and I. Kalvinsh, *J. Chem. Soc., Perkin Trans. 1*, 1999, 3527.
25 J. S. Yadav, B. V. Subba Reddy, G. G. K. S. Narayama Kumar and G. Madhusud han Reddy, *Tetrahedron Lett.*, 2007, **48**, 4903.
26 M. Mukhopadhyay and J. Iqbal, *J. Org. Chem.*, 1997, **62**, 1843.
27 M. Mukhopadhyay, M. Madhava Reddy, G. C. Maikap and J. Iqbal, *J. Org. Chem.*, 1995, **60**, 2670.
28 A. Tarlani, A. Riahi, M. Albedini, M. M. Amini and J. Muzart, *J. Mol. Catal. A: Chem.*, 2006, **260**, 187.
29 H. Firouzabadi, N. Iranpoor and A. Khoshnood, *Catal. Commun.*, 2008, **9**, 529.
30 S. Top and G. Jaouen, *J. Org. Chem.*, 1981, **46**, 78.
31 F. Tamaddon, M. Khoobi and E. Keshawarz, *Tetrahedron Lett.*, 2007, **48**, 3643.
32 Z. Habibi, P. Salesi, M. A. Zolfigol and M. Yousefi, *Synlett*, 2007, 812.
33 V. Polshettiwar and R. S. Varma, *Tetrahedron Lett.*, 2008, **49**, 2661; T. Maki, K. Ishihara and H. Yamamoto, *Org. Lett.*, 2006, **8**, 1431.
34 Z. D. Wang, S. O. Sheikh, S. Cox, Y. Zhang and K. Massey, *Eur. J. Org. Chem.*, 2007, 2243; J. C. Brandt, S. C. Elmore, R. I. Robinson and T. Wirth, *Synlett*, 2010, 3099.
35 A. Garcia Martinez, R. Martinez Alvarez, E. Teso Vilar, A. Gracia Fraile, M. Hanack and L. R. Subramanian, *Tetrahedron Lett.*, 1989, **30**, 581.
36 D. Djaidi, R. Bishop, D. C. Craig and M. L. Scudder, *J. Chem. Soc., Perkin Trans. 1*, 1996, 1859; P. Rubenbauer and T. Bach, *Chem. Commun.*, 2009, 2130.
37 M. D. Santos, B. Crousse and D. Bonnet-Delpon, *Tetrahedron Lett.*, 2009, **50**, 857.
38 Congjizha, R. G. Atkins and A. F. Masters, *J. Sol-Gel Sci. Technol.*, 1998, **13**, 103.
39 L. Boroica, D. Radu and R. Medianu, *J. Optoelectronics & Advanced Materials*, 2008, **10**, 3217.
40 R. L. Siqueira, I. V. P. Yoshida, L. C. Pardini and M. A. Schiavon, *Mater. Res.*, 2007, **10**, 147.
41 M. A. Zolfigol, *Tetrahedron*, 2001, **57**, 9509.
42 E. Callens, A. J. Burtonb and A. G. M. Barretta, *Tetrahedron Lett.*, 2006, **47**, 8699.
43 J. C. Baum, J. E. Milne, J. A. Murry and O. R. Thiel, *J. Org. Chem.*, 2009, **74**, 2207.
44 P. Theerthagiri, A. Lalitha and P. N. Arunachalam, *Tetrahedron Lett.*, 2010, **51**, 2813.
45 B. Anxionnat, A. Guerinot, S. Reymond and J. Cossy, *Tetrahedron Lett.*, 2009, **50**, 3470.
46 M. Barbero, S. Bazzi, S. Cadamuro and S. Dughera, *Eur. J. Org. Chem.*, 2009, 430; B. M. Choudary, S. Madhi, M. L. Kantam, B. Sreedhar and Y. Iwasawa, *J. Am. Chem. Soc.*, 2004, **126**, 2292; B. M. Choudary, S. Madhi, M. L. Kantam, B. Sreedhar and Y. Iwasawa, *J. Am. Chem. Soc.*, 2004, **126**, 6833.